

## N O T I C E

THIS DOCUMENT HAS BEEN REPRODUCED FROM  
MICROFICHE. ALTHOUGH IT IS RECOGNIZED THAT  
CERTAIN PORTIONS ARE ILLEGIBLE, IT IS BEING RELEASED  
IN THE INTEREST OF MAKING AVAILABLE AS MUCH  
INFORMATION AS POSSIBLE

(NASA-TM-80685) LARGE ANTENNA  
MULTIFREQUENCY MICROWAVE RADIOMETER (LAMMR)  
SYSTEM DESIGN (NASA) 33 p HC A03/MF A01  
CSCL 14B

N80-27675

Unclas  
25202  
G3/35



Technical Memorandum 80685

# Large Antenna Multifrequency Microwave Radiometer (LAMMR) System Design

J. L. King

MAY 1980



National Aeronautics and  
Space Administration

**Goddard Space Flight Center**  
Greenbelt, Maryland 20771

TM 80685

**LARGE ANTENNA MULTIFREQUENCY MICROWAVE  
RADIOMETER (LAMMR) SYSTEM DESIGN**

**J. L. King**

**May 1980**

**GODDARD SPACE FLIGHT CENTER  
Greenbelt, Maryland 20771**

**LARGE ANTENNA MULTIFREQUENCY MICROWAVE  
RADIOMETER (LAMMR) SYSTEM DESIGN**

**J. L. King**

**ABSTRACT**

The Large Antenna Multifrequency Microwave Radiometer (LAMMR) is a high resolution 4 meter aperture scanning radiometer system designed to determine sea surface temperature and wind speed, atmospheric water vapor and liquid water, precipitation and various sea ice parameters by interpreting brightness temperature images from low earth orbiting satellites. One version of this system with 7 channels dual polarized from 4.3 to 36.5 GHz is now included in the National Oceanic Satellite System (NOSS) which has a planned launch in 1986. The LAMMR with dual linear horizontal and vertical polarization radiometer channels from 1.4 to 91 GHz can provide multidiscipline data with resolutions from 105 to 7 km which is a factor of 5 better than were achieved on the Nimbus and Seasat Scanning Multichannel Microwave Radiometers (SMMR).

Trade-off studies have selected a mechanically scanned (1 rps) offset parabolic reflector with prime focus clustered feed optics which, for the purposes of this TM, is the baseline concept to implement the multichannel measurements. The scan mechanism must provide momentum compensation and power/data transfer functions for the sensor. The LAMMR design must also consider the antenna system and radiometer electronics mass distribution in order to achieve the dynamic balance required to make this instrument compatible with the free flyer spacecraft which must also accommodate other high resolution sensors. This dynamic balance criterion was a factor in the selection of the prime focus design over the Cassegrain approach. The earth viewing spillover energy and complex feed development required in the Cassegrain system was a second important factor. The 1 revolution per second scan rate required for contiguous coverage of the 7.2 km resolution beams

places stringent requirements on the reflector stiffness. In these studies, graphite epoxy with aluminum honeycomb was found to meet the tight surface tolerance requirements under spin and space thermal environments. Reflector surface tolerances in the  $5 \times 10^{-3}$  cm to  $25 \times 10^{-3}$  cm rms range have been predicted by NASTRAN models. Antenna pattern performance has also been modeled which shows the feasibility of achieving 90% beam efficiencies with these tolerances which is critical to radiometer system performance.

The LAMMR baseline radiometer system uses total power radiometers to achieve  $\Delta T$ 's in the .5 to 1.7°K range and system calibration accuracies in the 1-2°K range. A cold sky horn/ambient load two point calibration technique is used in this baseline concept and the second detector output uses an integrate and dump circuit to sample the scanning cross-track resolution cells.

The concepts expressed in this Technical Memorandum represent the conclusions of the author. Endorsement by the NOSS Project is neither expressed nor implied. Specific NOSS requirements may dictate selection of a concept not represented in this document.

## CONTENTS

	<u>Page</u>
ABSTRACT .....	iii
I. INTRODUCTION .....	1
II. LAMMR OVERALL SYSTEM APPROACH AND REQUIREMENTS .....	4
III. LAMMR RADIOMETER SUBSYSTEM .....	12
IV. LAMMR ANTENNA SUBSYSTEM .....	22
V. CONCLUSION .....	25
ACKNOWLEDGEMENTS .....	27
REFERENCES .....	27

## TABLE

<u>Table</u>	<u>Page</u>
1 LAMMR Geophysical Measurement Goals .....	3

## LIST OF ILLUSTRATIONS

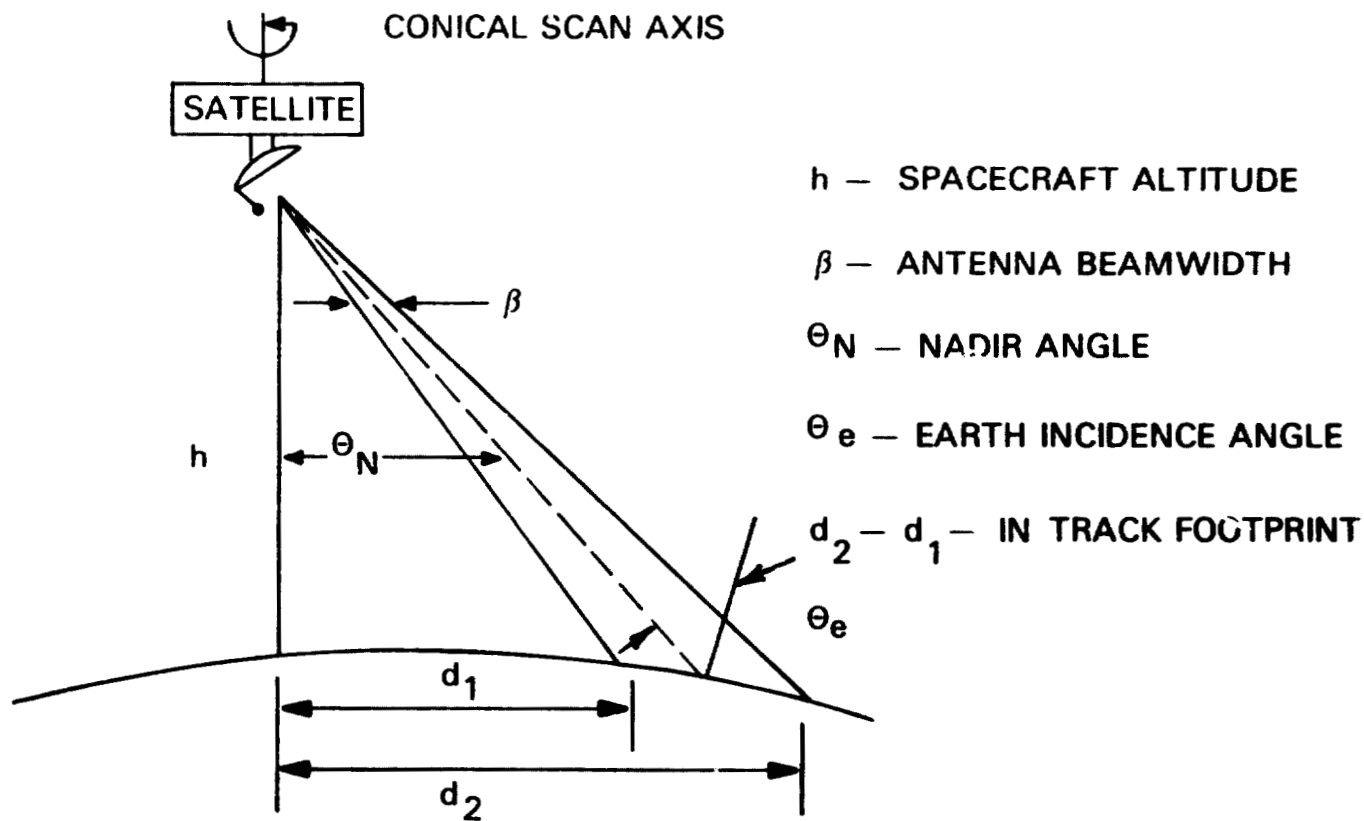
<u>Figure</u>	<u>Page</u>
1 LAMMR System Geometry .....	2
2 Radiometric Channel Parameter Sensitivity .....	5
3 System Scan Geometry .....	8
4 Radiometer Sensitivity Determinations .....	11
5 LAMMR System Configuration .....	13
6 LAMMR Radiometer System Configuration .....	14
7 Radiometer System Temperature - $T_s$ .....	15
8a Layout of 3 dB IFOV's on Ground Due to Offset Beams .....	17
8b LAMMR Beam Scan Overlap .....	18
9 LAMMR Data Rate Determination .....	19
10 LAMMR Antenna Geometry .....	23
11 LAMMR Antenna System Requirements .....	26

# LARGE ANTENNA MULTIFREQUENCY MICROWAVE RADIOMETER (LAMMR) SYSTEM DESIGN

## I. INTRODUCTION

The LAMMR is a multichannel microwave radiometer system designed to measure brightness temperatures to determine sea surface temperature (SST), sea surface wind speed (SSWS), atmospheric water vapor, liquid water, precipitation, and sea ice parameters (type, concentration) from low earth orbiting satellites. The 4 meter aperture antenna system is conically scanned at one revolution per second with a mechanical subsystem to produce global maps of these geophysical parameters with earth resolution elements (in-track footprints) from 105 to 7.2 kilometers depending on the lowest frequency used for a particular parameter (see Figure 1). This system, with the inclusion of 5.1 and 6.6 and without the 1.4 and 91 GHz channels, is now planned as part of the National Oceanic Satellite System (NOSS) sensor payload scheduled for launch in 1986. This sensor will achieve resolutions approximately five times better than were achieved by the Nimbus and Seasat passive microwave sensors such as the Electrically Scanned Microwave Radiometer (ESMR) and the Scanning Multichannel Microwave Radiometer (SMMR) which first demonstrated these measurements from space. The LAMMR, because of better spatial resolution, and wider swath coverage (1360 km vs approximately 800 km for SMMR), will improve the accuracy and temporal coverage of these measurements to meet the goals outlined in Table 1. The better resolution of the sea surface temperature (SST) measurement has another important by-product. The percentage of measured ocean area increases from approximately 80% for SMMR with 150 km resolution to approximately 94% for LAMMR with 36 km resolution because the SST measurements which include partial land/sea surfaces (coast lines and island areas) in the field of view must be thrown out due to the large unknown land temperature effects.

The following sections will describe the LAMMR system design approaches which have been studied by GSFC, JPL, General Electric (GE), and Aerojet Electro Systems (AES) over the past two years. Present plans are for one LAMMR system to be procured for NOSS by the Government in a



$h$  – SPACECRAFT ALTITUDE

$\beta$  – ANTENNA BEAMWIDTH

$\theta_N$  – NADIR ANGLE

$\theta_e$  – EARTH INCIDENCE ANGLE

$d_2 - d_1$  – IN TRACK FOOTPRINT

FREQUENCY GHz	1.4	4.3	10.65	18.7	21.3	36.5	91
$\beta$ - DEGREES	3.8	1.3	0.6	0.3	0.26	0.26	0.26
$(d_2 - d_1)$ KM	106	36	16	8.3	7.2	7.2	7.2

NOTE:  $h = 700$ KM

SATELLITE SUBTRACK VELOCITY 6.75KM/SEC

Figure 1. LAMMR System Geometry



**Table 1**  
**LAMMR Geophysical Measurement Goals**

<u>PARAMETER</u>	<u>ACCURACY</u> RELATIVE ABSOLUTE		<u>RANGE</u>	<u>RESOLUTION</u> KM	<u>PRIMARY CHANNELS</u>
<u>SEA SURFACE TEMP.</u>	.5	1 <sup>o</sup>	- 2 TO 35°C	36, 25	4.3, 10.65, 6.8
<u>SEA SURFACE WIND SPEED</u>	1	2	7 - 50 M/S	17 KM	10.65, 18.7
<u>SEA ICE</u>					
% OF AREA	2	5	0 - 100%	7	18.7
TYPE	NEW, 1ST YEAR, MULTIYEAR			8	18.7, 36.5
SURFACE MELT ICE SHEET	WET/DRY			7	36.5, 91
SUB SURFACE TEMPERATURE	1 <sup>o</sup>	1 <sup>o</sup>	-10 TO +5°C	106	1.4
<u>PRECIPITATION</u>					
OVER OCEAN	FACTOR OF 2		1-20MM/HR	8	18.7
OVER LAND	YES/NO		> 1MM/HR	7	36.5, 91
<u>SNOW</u>					
COVER	- 5%		0 - 100%	7	36.5, 91
% WATER CONTENT	RESEARCH ITEM		1 - 100CM	7	91
<u>ATMOSPHERE</u>					
WATER VAPOR	0-15 G/CM <sup>2</sup>		0-6G/CM <sup>2</sup>	7	18.7, 21.3
LIQUID WATER	4MG/CM <sup>2</sup>		0-100MG/CM <sup>2</sup>	8	21.3, 36.5

NOTE: SWATH 1361KM FROM A 700KM ORBIT RESULTS IN ~ 2 MEASUREMENTS PER DAY OVER MOST OF THE GLOBE

competitive procurement during 1980/81. The reader is cautioned that the LAMMR final system design may not use the approaches discussed in this paper because the interface constraints will be different. These discussions represent the GSFC LAMMR team's baseline LAMMR design based on these contractual studies with GE and AES and GSFC in-house analysis.

## II. LAMMR OVERALL SYSTEM APPROACH AND REQUIREMENTS

Radiometer channel selection becomes the first major system decision which drives the engineering tradeoffs involved in the LAMMR system design. The number of channels, polarization, and frequency is determined by the measurement objectives of the sensing system. The radiometric sensitivities to various parameters which dictate channel selection is shown in Figure 2. The measurement objectives given in Table 1 include ocean, weather, cryospheric and hydrological discipline objectives and frequencies from 1.4 to 91 GHz are required. The NOSS program objectives include only ocean and sea ice parameters and therefore the 1.4 and 91 GHz channels are deleted in the present NOSS baseline system. The radiometric brightness temperature algorithms require widely spaced channels to measure the surface roughness and atmospheric absorption variations as a function of frequency in order to separate the effects. For example, the atmospheric (water vapor, liquid water) and surface foam and roughness effects must be separated from the sea surface temperature measurement in order to reduce the SST measurement errors to acceptable levels. These radiometric parameter sensitivities (Figure 1) are not narrow band, sharp cut off responses, consequently most channels depend on more than one parameter. Thus a multichannel inversion matrix is used to improve the geophysical parameter measurement accuracy. The difference in the H and V polarization  $T_{\text{B}}$ 's are used to detect surface roughness and surface emission properties.

The channel frequency and bandwidth selection is also governed by a very practical consideration known as radio frequency interference (RFI). These spaceborne systems must operate in bands where interfering transmitter power is limited to a -155 to -165 dBW at the input to the radiometer depending on the particular application and radiometer sensitivity required. These channel sharing criteria and allocations are set by international agreements made at the World Administration Radio

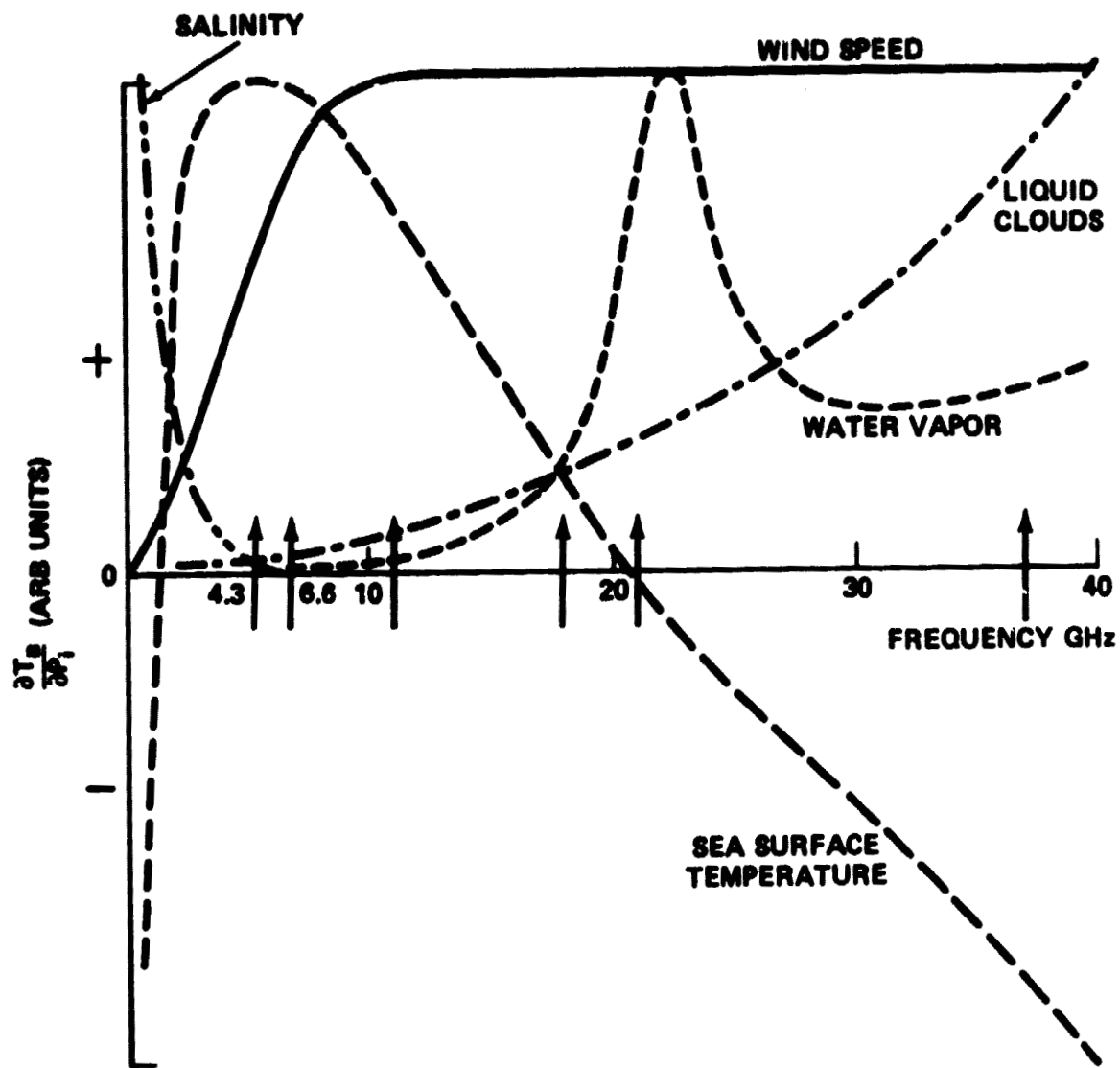


Figure 2. Radiometric Channel Parameter Sensitivity

Conferences (1979). The LAMMR channels shown in this report are in bands which meet these criteria except for the 6.6 GHz band listed under sea surface temperature (SST) in Table 1. This 6.6 GHz channel was flown on the Nimbus-7 and Seasat SMMR's. From reduction of some small amount of SMMR data, it appears in some regions of the world there may be interference in the 6.6 GHz channel as predicted. The exact effect on the coastal SST measurements has not yet been determined, but the strong desire to improve the LAMMR's SST spatial resolution from 36 km to 25 km (using 6.6 GHz) has made this an important issue. An analysis of the Nimbus SMMR data will be made to determine where the RFI contamination is severe. The 6.6 GHz and 5.1 GHz channel parameters are not presently shown in the rest of this report.

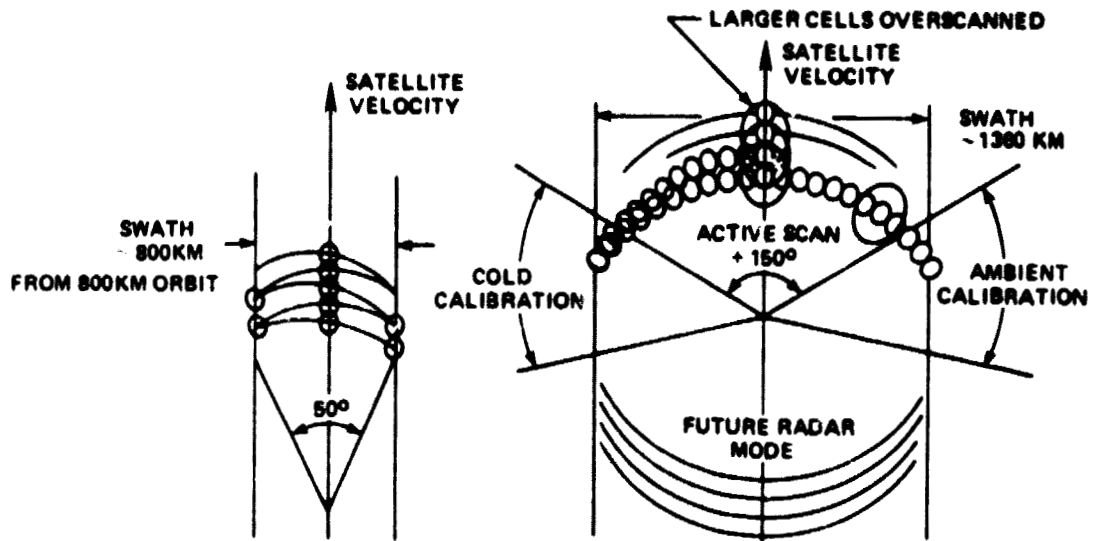
The LAMMR antenna type was another major trade-off decision required in the hardware system design phase. Possibilities range from multiple electrically scanned phased arrays to various reflector system approaches. The electrically scanned arrays were discarded early in the design because of the need to develop separate antennas at all of the LAMMR channels (1.4, 4.3, 10.65, 18.7-21.3, 36.5, and 91 GHz) except possible 18.7 and 21.3 GHz where a single array design was proposed. The arrays of this size (approximately 4 meter aperture) also have significant RF losses which make .5-1.0°K calibration accuracies and  $\Delta T$  temperature sensitivities very difficult if not impossible, to achieve. These two negative factors in turn lead to much higher overall system cost estimates, and the mechanically scanned reflector with inherently wideband performance was selected as the LAMMR antenna approach.

Several mechanically scanned reflector system configurations were studied. One approach proposed by JPL was an offset parabolic torus with mechanically scanned feeds located on a large wheel. This had the advantage of not scanning the main reflector, but the feeds only viewed a section of the reflector surface at any one time which required the parabolic torus reflector to be 2-3 times larger in the scan dimension than a single offset parabolic reflector. The requirement for a 4 meter effective aperture to meet measurement goals and the approximately 4 meter shuttle

launch diameter constraint made a shuttle launched parabolic torus (8-12 meter size) on a free flyer impractical because of the complex deployments or space assembly required. A joint user/university/NASA study group chaired by Professor David Staelin of M.I.T. reviewed all of these approaches and selected the single offset parabolic reflector as the recommended LAMMR baseline design in 1978. This left the offset parabolic reflector multifrequency feed design open to tradeoffs between prime focus and Cassegrain approaches which will be discussed in section IV on the antenna subsystem.

The LAMMR antenna scan geometry was the next required system design decision. In the past, both through-nadir cross-track (ESMR-5) and conically scanned (SMMR) systems had been flown. The through-nadir scanned systems provide better resolution over most of the scan for a given size aperture because of the shorter path length near nadir. The problems with this type of scan occur in interpreting the variable beamwidth, polarizations, and incidence angles of each resolution element across the scan track. The physics of the interpretation of the brightness temperatures becomes much simpler over the ocean at a constant earth incidence angle of approximately  $50^\circ$  where the ocean surface emissivity is 30% higher than at nadir and the vertical polarization is nearly independent of windspeed.<sup>1,2</sup> The dual polarized multifrequency brightness temperatures are necessary at many frequencies to be able to separate the various frequency dependent effects of ocean roughness, ocean temperature, atmospheric absorption and wind generated foam used in the interpretative models as shown in Figure 2. These factors dictate that the system be conically scanned with an earth incidence angle of about  $50^\circ$ .

The types of conical scan can be either constant speed or variable with  $360^\circ$  rotation or zigzag scan motions (Figure 3). The Nimbus SMMR was able to use a zigzag ( $\pm 25^\circ$ ) sinusoidal rate scan mechanism due to the relatively low mass (approximately 4 kg) and slow scan rate (4 sec) of the 80 cm diameter (Figure 2a) reflector. However, even with this small lightweight reflector, a complex momentum compensation mechanism was required to meet the low residual torque specification required by the Nimbus spacecraft. This zigzag scan approach has the benefit of maximizing the time the sensor spends looking at the desired scene (integration time). The LAMMR system designers,



A. SMMR ZIG ZAG SCAN (TOP VIEW)

B. LAMMR 360° SCAN (TOP VIEW)

256 CELLS ACROSS SCAN AT 10.65 GHz  
AND ABOVE; 128 CELLS AT 4.3 GHz

C. THE IN-TRACK RESOLUTION ELEMENT IS DETERMINED BY THE 3 dB ANTENNA BEAMWIDTH AND THE CROSS TRACK RESOLUTION ELEMENT IS DETERMINED BY THE INTEGRATION PERIOD OF THE CELL.

CHANNEL	CELL DIMENSION KM		CELLS/150° SCAN WITH XT - IT	2 <sup>N</sup> CELL/150° SCAN
	X-TRACK	IN-TRACK		
4.3	14.4	36.	51	128
10.65	7.2	17.	108	256
18.7	7.2	8.3	222	256
21.3	7.2	7.2	256	256
36.5	7.2	7.2	256	256
OPTIONAL	1.4	57.5	17	32
	91.	7.2	256	256

\* ASSUMES 700KM ORBIT AND 50° EARTH INCIDENCE ANGLE

Figure 3. System Scan Geometry

however, chose 360° continuous rotation for the scan mechanism because of the large mass of the scanning antenna and rapid scan rate required (Figure 3b). This continuous constant velocity scan motion used on the LAMMR tends to minimize the variable mechanical torques on the reflector and host spacecraft. This is important for the reflector because of the tight surface tolerances (2-10 mils) required to operate up to 36.5 and 91 GHz and for the NOSS so that other high resolution sensors are not perturbed by the LAMMR's motion.

The continuous 360° LAMMR scan period is divided into segments of active radiometric measurements, ambient and cold calibration cycles, and an unused segment in the rear viewing segment of the scan which may be used to operate in a radar mode on future missions. The 150° active scan segment was selected as a compromise between maximum swath (180° segment) and minimum system data rate. The 150° segment provides 96% of the 180° maximum swath (1361 km vs 1410 km) while saving a 17% increase in data rate. The cells near the edge of the swath are oversampled in-track due to the overlapping of the cells which move nearly parallel to the satellite ground track as can be seen qualitatively in Figure 3b.

This conical scan motion must then be defined in terms of the radiometric channels resolution cells (Figure 2c). The channel resolutions given in Figure 1 are the 3 db in-track energy contours of the scanning antenna beams. The cross-track 3 db beamwidth would provide ground resolution contours which are narrower than these values by an approximately 1.6 ratio. This elliptical 3 db ground footprint is difficult to deal with when using square lat/longitude grids in the retrieval algorithms. Therefore, the scientists prefer a circular or square cell definition which represents the best average brightness temperature within each cell. To accomplish this in the LAMMR sensor, the cross-track cell is spatially filtered to equal the in-track 3 db cell dimension given in Figure 1. This results in from 51 to 256 cross-track resolution elements in the 1842 kilometer sector length of the 150° active scan region of LAMMR (Figure 2b). The number of these elements were increased where necessary to the next highest  $2^N$  number of cells to facilitate the use of FFT processing techniques on the ground during data reduction. The 4.3 and 10.65 GHz channels are sampled at least twice per

resolution element to satisfy the Nyquist sampling criteria for these channels. This was not done at the higher frequency channels in this baseline system because of the required increase in the LAMMR data rate (Figure 3c). Once the data system impact of the higher data rate is known, the sample rates of the 256 cell channels may be increased.

The time it takes the beam to scan cross track the in-track distance given in Figure 1 is the integration time used to calculate the RMS temperature sensitivity  $\Delta T$  in Figure 4. The temperature sensitivity  $\Delta T$  is usually specified for a particular cell and integration time during a single scan, and the scan rate is set to provide contiguous in-track 3 db contour cell coverage at the highest resolution of the sensor. For LAMMR, the scan period is determined by the 7.2 km resolution divided by 6.74 km/sec, the satellite sub-track velocity from 700 km altitude, which equals 1.07 sec. The actual LAMMR scan rate was chosen to be 1 revolution per second to allow for slightly lower orbit operation and slightly narrower beamwidths which could result at 36.5 and 91 GHz (discussed in upcoming antenna section). In the case of the larger cells (4.3 and 10.6 GHz) which are being scanned cross-track at a much higher rate than necessary, several in-track cells are averaged together in the ground processing to achieve a  $\Delta T$  only slightly higher than would be possible if the antenna was scanned at the slower rate compatible with their resolution.

The temperature sensitivities of each radiometric channel are given in Figure 4. The use of total power radiometer techniques are assumed in these calculations with a 5% reduction in  $\Delta T$  allowed for finite calibration source sampling errors (i.e., about X10 cell integration periods for each ambient and cold temperature calibration per 1 second scan). The  $\frac{\Delta G}{G}$  fluctuations are assumed negligible ( $>1 \times 10^{-4}$ ) for the 1 second calibration cycle and 1.63 to 13 milliseconds integration periods used in the LAMMR. The integration times are specified for a single one second scan period for the number of cells given in Figure 3c. The averaged temperature sensitivities are also given which assumes a processing scheme in which the oversampled individual cells will be averaged over the resolutions given in the last column of Figure 4. The equivalent system noise temperature  $T_s$  calculations will be explained later in the radiometer subsystem section. Figure 4 shows that LAMMR has  $\Delta T$



## I. RADIOMETER SENSITIVITY DETERMINATIONS

$$\Delta T_{\text{RMS}} = \frac{K T_s}{\sqrt{BW \times T + \left(\frac{\Delta G}{G}\right)^2}}$$

$T_s$  = EQUIVALENT INPUT NOISE TEMPERATURE IN ° KELVIN OF RADIOMETER INCLUDING RECEIVER, ANTENNA, AND LOSS CONTRIBUTIONS REFERENCED TO ANTENNA INPUT; ASSUME RADIOMETRIC TARGET TEMP 200°K

$K$  = RADIOMETER TYPE FACTOR i.e.,  $K=1$  FOR THEORETICAL TOTAL POWER AND 2 FOR SQUAREWAVE MODULATED DICKE RADIOMETER; USE 1.05 FOR LAMMR

$BW$  = PREDETECTION RF BANDWIDTH IN Hz i.e.,  $BW = \frac{1}{2}$  RF BANDWIDTH IN SUPER HETRODEYNE DOUBLE SIDEBAND RADIOMETER AND  $BW =$  RF BANDWIDTH IN A TUNED RF AMPLIFIER TYPE OF RADIOMETER

$\frac{\Delta G}{G}$  = RMS RECEIVER POWER GAIN FLUXUATIONS; ASSUME  $10^{-4}$  (NEGLIGIBLE) FOR LAMMR SYSTEM

$T$  = INTEGRATION TIME, SECONDS – ASSUMING NEGLIGIBLE A/D CONVERSION AND DUMP TIME

II. CHANNEL GHz	BW $10^6$ Hz	$T_s$ °K	SINGLE SCAN T $10^{-3}$ SEC	SINGLE SCAN $\Delta T$ °K	AVERAGED $\Delta T$ OVER IFOV °K	RESOLUTION IFOV CROSSTRACK=IN-TRACK KM
* 1.4	28	363	13.	.63	0.06	106
* 4.3	200	340	3.26	.44	.14	36
* 10.65	100	697	1.63	1.81	.77	17
18.7	100	624	1.63	1.62	1.40	8.3
21.3	100	639	1.63	1.66	1.66	7.2
36.5	500	666	1.63	.78	.78	7.2
91.0	1000	1300	1.63	1.1	1.1	7.2

TRF\*

Figure 4. Radiometer Sensitivity Determinations

temperature sensitivities from .06 to 1.66 over the averaged IFOV's, these sensitivities are near the maximum allowable to be able to meet the measurement objectives given in Table 1 and radiometer system performance near the state of the art has been assumed. The following sections of this report will cover the radiometer and antenna subsystems in more detail based on the system requirements and approaches described in this section.

### III. LAMMR RADIOMETER SUBSYSTEM

The radiometer subsystem with channels from 1.4 to 91 GHz can be accommodated on the LAMMR scanning antenna subsystem. The 1.4 and 91 GHz channels are options on the NOSS LAMMR but power and signal transfer capability in the antenna's scan mechanism can be designed to accommodate these extra channels and the basic structure can also be designed to handle the extra weight. The majority of the radiometer subsystem will be located at the antenna's prime focus on the end of an approximately 3 meter feed arm which will be stowed during launch and deployed prior to sensor operation (Figure 5).

The radiometer system consists of the RF electronics, the calibration system (cold horns, ambient loads, switches) and the signal processor. The radiometer system performance can be summarized in terms of equivalent system temperatures ( $T_s$ ) which are used to calculate  $\Delta T$  in Figure 4.  $T_s$  is a function of system losses, input temperature, and receiver noise figures as shown in Figure 7. The types of radiometers shown in Figure 6 are all total power systems with a cold sky horn and ambient load calibration which are sampled many times per scan. The total power radiometers could be replaced by Dicke or noise injection null balanced radiometers at 1.4 GHz to save weight at the expense of doubling  $\Delta T$  which is not critical at 1.4 GHz. The TRF and superheterodyne RF approaches and signal processing system design in Figure 6 are only two of many configurations which could meet LAMMR requirements. This is only one of the many areas in which the final detailed design will probably differ from the design suggested in this TM. The lower frequency tuned radio-frequency (TRF) radiometers will probably use low noise FET amplifiers which provide maximum predetection noise bandwidth and lower noise figure (below 15 GHz) when compared to mixer

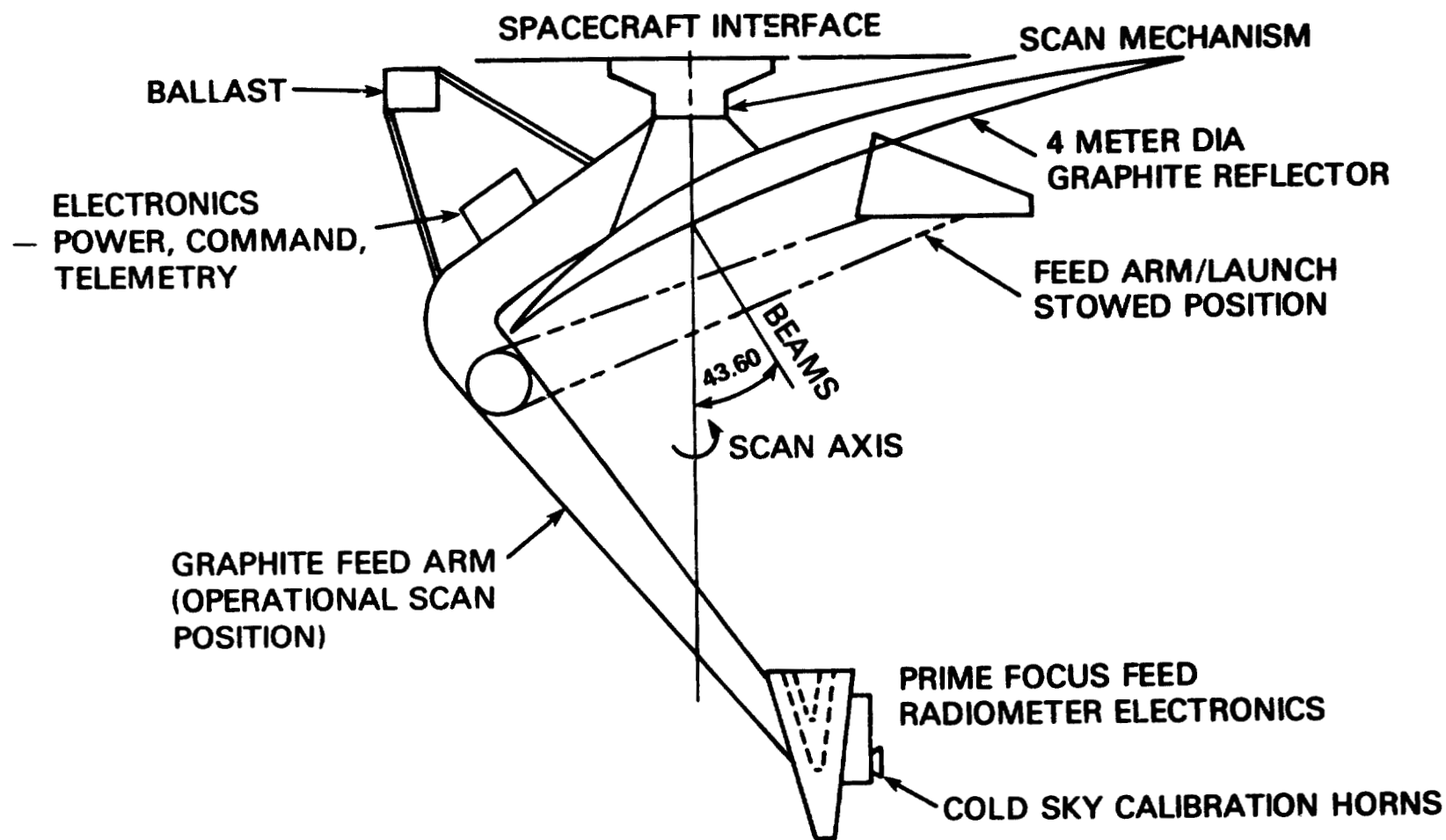


Figure 5. LAMMR System Configuration

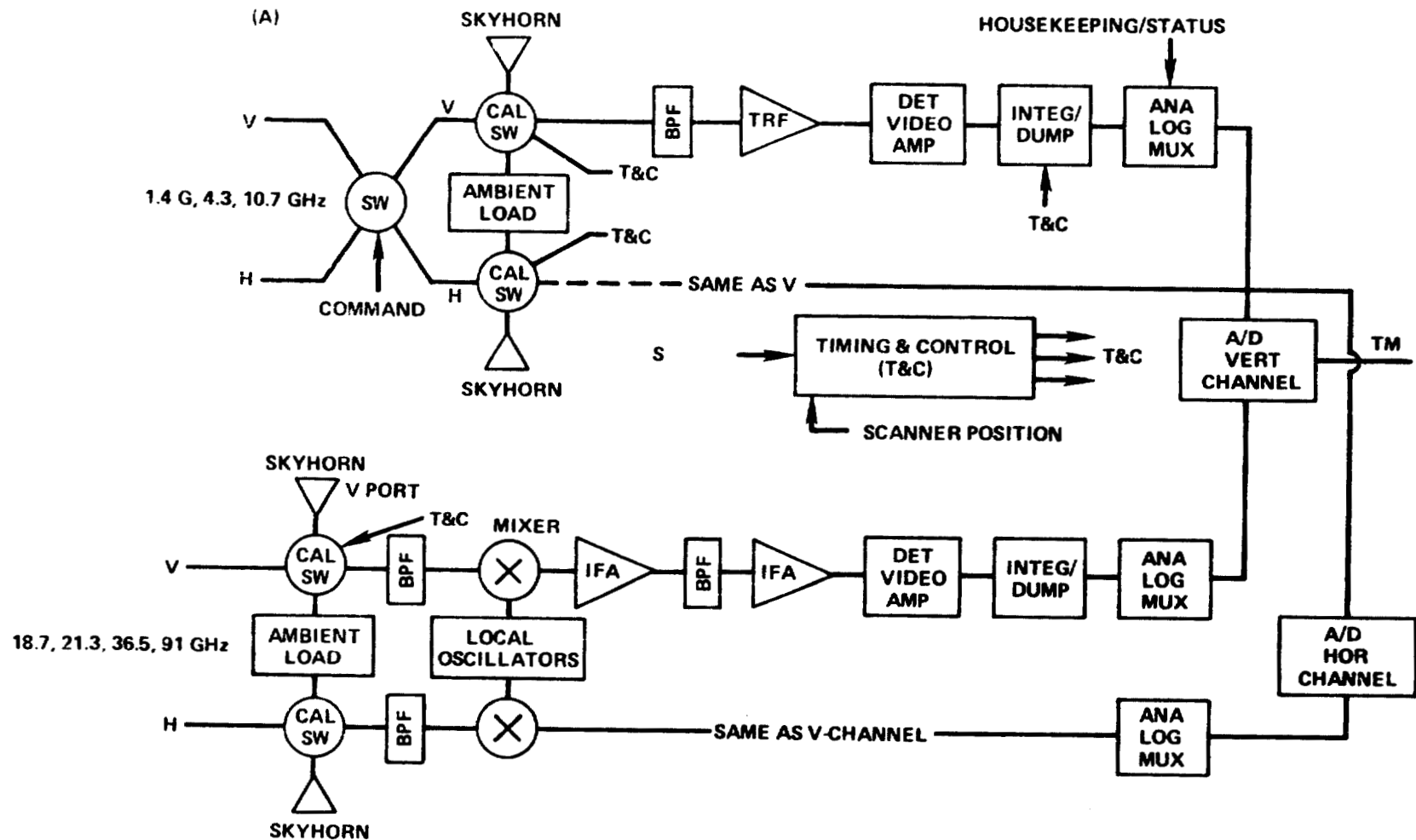


Figure 6. LAMMR Radiometer System Configuration

## B. EQUIVALENT SYSTEM TEMPERATURES REFERENCED TO ANTENNA INPUT

$$T_s = T_A + (1 - a) T_L + \frac{T_R}{a}$$

<u>CHANNEL</u> GHz	<u>a</u>	<u>T<sub>R</sub></u> K	<u>T<sub>S</sub></u> K
1.4	.871	110	363
4.3	.9	101	340
6.6	.85	170	443
10.7	.81	360	697
18.7	.79	290	624
21.3	.78	290	639
36.5	.74	290	666
91.0	.63	627	1301

**T<sub>A</sub> = 200 K ANTENNA INPUT TEMP.**

**T<sub>L</sub> = PHYSICAL TEMPERATURE OF  
LOSSES (290°K)**

**a = LOSS TRANSMISSION  
COEFFICIENT**

**T<sub>R</sub> = EQUIVALENT RECEIVER NOISE  
TEMPERATURE IN K**

Figure 7. Radiometer System Temperature - T<sub>S</sub>

approaches. The design of the bandpass filter to protect the radiometers from Radio Frequency Interference (RFI) near the selected channels becomes more difficult in TRF radiometers than in mixer systems where IF filtering at lower frequencies can be used. The LAMMR RFI out-of-band system rejection specification of 30 db down 30 MHz (21.3 GHz channel and below) from the radiometer channels band edge (3 db points) was selected to protect the radiometers from RFI transmitter sidelobe and scattered radiation from ground sources. Direct line-of-sight transmission from a RFI source with antenna gain would require complex  $> 100$  db rejection filters which were not included in the baseline design because these direct RFI transmissions will cause problems for only a few resolution cells during a scan. This data can be identified and deleted during data processing. The TRF radiometers in Figure 6 also contain a polarization switch to enable either radiometer to be connected to either V or H polarization. This provides radiometer system redundancy in the primary sea surface temperature and wind speed measurements where  $\Delta T$  could be traded off by sharing a single radiometer between H and V channels in case of a single radiometer failure. The polarization switches are not included in the higher frequency channels because of the added switch losses and because the channels themselves are somewhat redundant in determining their primary geophysical parameters with slightly degraded accuracy. The super-heterodyne systems will probably use low noise balanced mixers with Schottky barrier gallium arsenide diodes operated in a double sideband configuration with a Gunn diode local oscillator in the center of the RF channel. The IF amplifiers will have bandwidths from approximately 500 kHz out to the specified predetection 3 db bandwidths. The video detectors and amplifiers are linear power versus voltage devices. The design of the channel analog multiplexer, timing, and control circuits, and analog to digital converters are shown in a configuration which uses one A/D converter per polarization which is shared in time between the various channels to cause the channel data to be recorded with nearly coincident beam centers overlaid on the 256 or 128 cross-track scan grid (Figure 8). The beams will not be precisely coincident because of the in-track satellite motion which will take place between the spatially separated beam centers. The resultant LAMMR data rate is given in Figure 9 along with a list of typical telemetry data needed to calibrate the radiometer system.

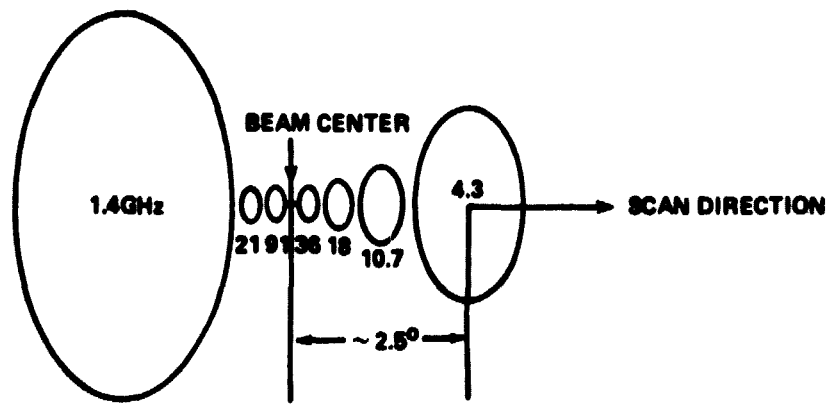
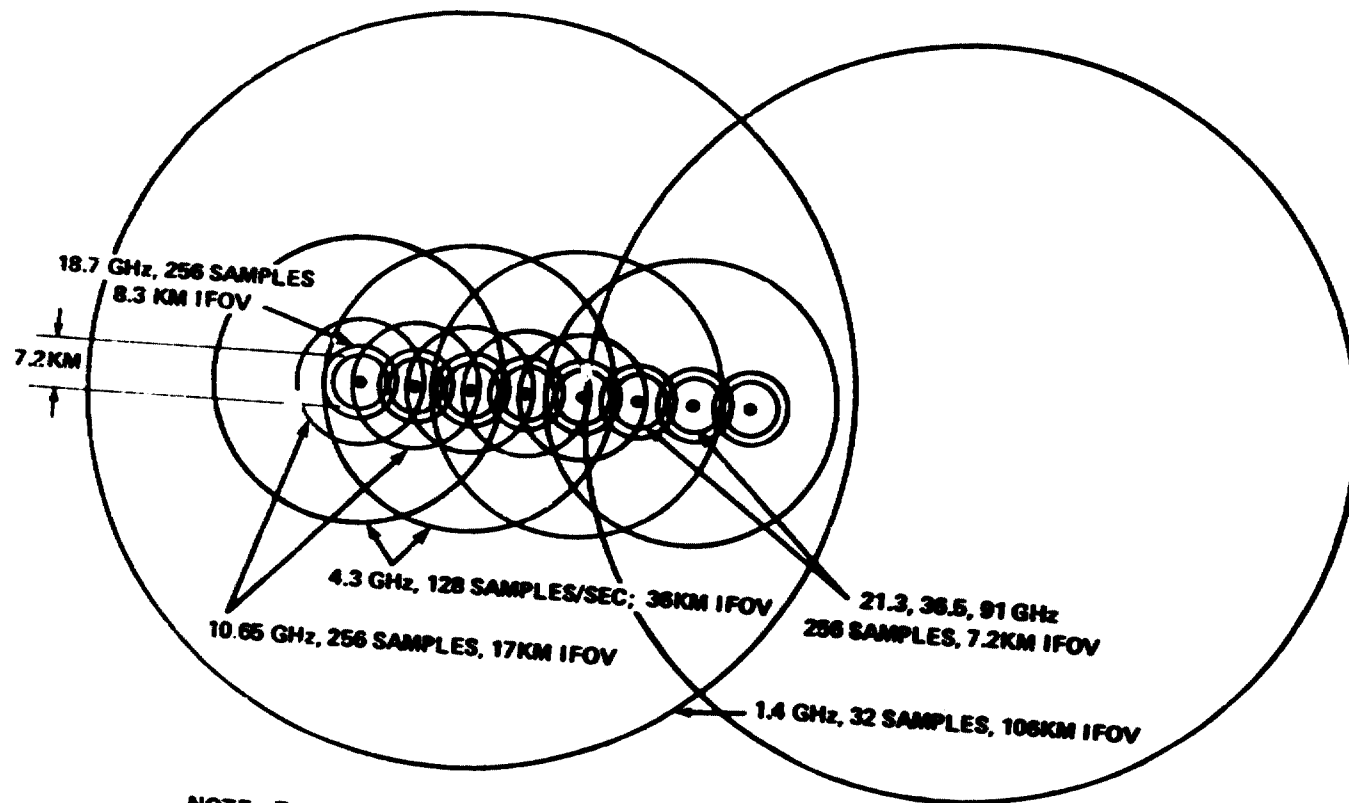


Figure 8a. Layout of 3 dB IFOV's on Ground Due to Offset Beams

TIME DELAYED OVERLAY OF CIRCULAR CELLS ON SINGLE SCAN



NOTE: THE CELLS ARE SAMPLED IN EQUAL SENSOR SCAN ANGLE SEGMENTS OF  $\sim .58^\circ$ .  
THE TOTAL  $150^\circ$  SWATH SEGMENT LENGTHS ON THE EARTH IS 1842KM FROM A  
700 KM ORBIT.

Figure 8b. LAMMR Beam Scan Overlap



CHANNELS	NUMBER OF SAMPLES PER 150° SCAN SEGMENT	NUMBER OF BITS/SAMPLE	CALIBRATION SAMPLES OF T <sub>COLD</sub>	CALIBRATION SAMPLES OF T <sub>AMBIENT</sub>	DATA RATE KGS
V&H 1.4	32	12	16	16	1,536
V&H 4.3	128	12	↓	↓	3,840
V&H 10.65	256	12			6,912
V&H 18.7					6,912
V&H 21.3					6,912
V&H 36.5					6,912
V&H 91.0	256	12			6,912
V&H 6.6	128	12			3,840
					<b>TOTAL</b>

16

**SYSTEM STATUS/HOUSEKEEPING DATA**

6 - AZIMUTH POSITION READOUTS 12 BITS	= 72 B/SEC
6 - 14 BITS TEMPERATURE READOUTS PER CHANNEL 16x14x6	= 1,344 B/SEC
2-16 BIT STATUS WORDS UPDATED EVERY 4 TIME/SEC	= 128 B/SEC
MISC. VOLTAGES, SCANNER RATE, ETC. 10 x 12 BITS	= 120 B/SEC
	<u>1,664 B/SEC</u>

**TOTAL SENSOR DATA RATE - 45,440 B/SEC**

**NOTE: THIS DATA RATE DOES NOT SAMPLE THE 3dB CROSS TRACK RESOLUTION CELLS TO MEET A NYQUIST CRITERIA AT FREQUENCIES ABOVE 10.65 GHZ. A SMEARING OF THE 3dB RESOLUTION CELLS EQUAL TO THE ALONG TRACK (SATELLITE SUBTRACK) RESOLUTION DIMENSION IS ALLOWED AT THE HIGHER FREQUENCIES TO LIMIT THE DATA RATE.**

**Figure 9. LAMMR Data Rate Determination**

The LAMMR baseline in orbit calibration approach uses ferrite circulator switches to select a warm waveguide load termination or cold space horn ( $T_B \sim 3\text{ K}$ ) input to the radiometer. The radiometer measures the warm and cold calibration sources for several normal integration periods to minimize the noise in the computation of the radiometric gain factors (K/Volt) which are used to convert each channels' output voltage to brightness temperature. This radiometric gain factor must be updated often enough to prevent system gain changes from introducing errors in brightness temperature measurements. This period of time can range from  $\sim 1$  sec up to tens of seconds depending on the gain stability of the system which is also a function of temperature stability.

These warm load and cold sky horn output voltages are assigned equivalent brightness temperatures which depend on the losses and isolation between these sources and the input to the radiometer. These losses in the transmission line between the warm load termination and cold sky horn are distributed over lengths of waveguide, switches, isolators, coax lines, etc., which can have different physical temperatures. These components can also change their losses and isolation as a function of temperature which makes the calibration model very complex (reference NASA TM-80244, C. D. Calhoun, March 1979). These component variations as a function of temperature must be characterized over the temperature range expected in the radiometer's space configuration and thermal environment.

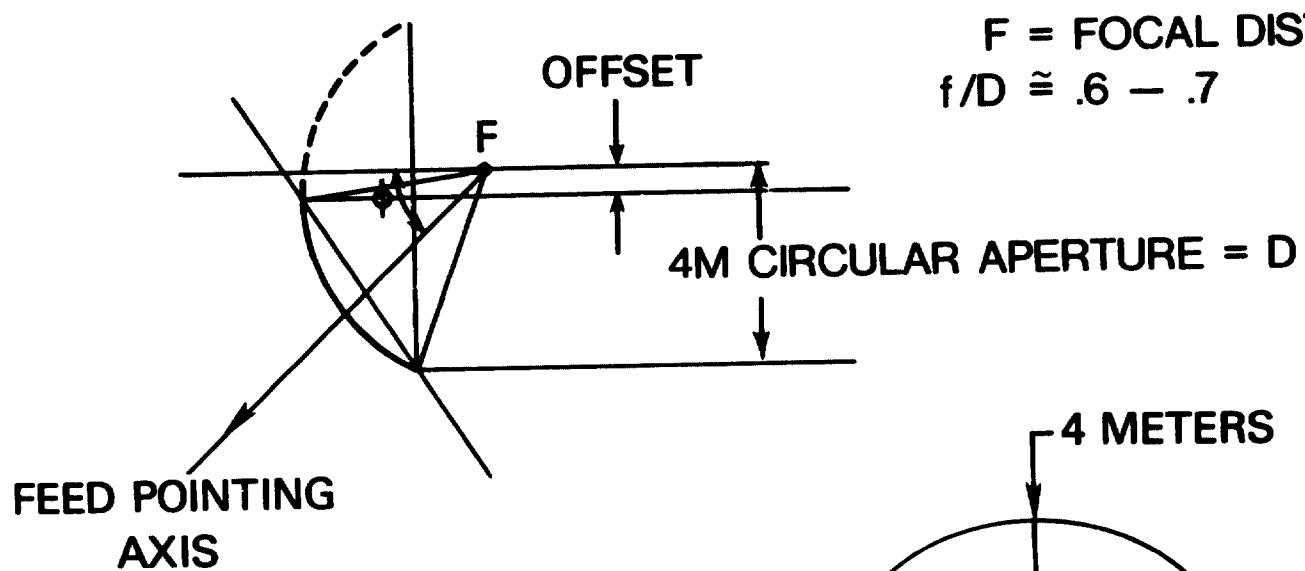
The calibration models typically use multi-element radiative transfer equations with regression analysis during the total system test (reference Stacey/SMMR). This requires the characterization of the components (waveguide, OMT, switches, filters, etc.) over the expected temperature ranges prior to the system thermal vacuum test. Using this component data, a rough calibration model can be formulated to predict the input calibration temperatures as a function of system physical temperatures. After these components are assembled into the flight radiometer configuration, the net losses and behavior of the total assembly will probably differ in performance from that predicted by the model. This is due to the way the coupling losses and VSWR's combine in the new assembly. This total radiometer assembly must then be tested over the expected temperature range in thermal

vacuum using the temperature monitors provided in the telemetry data on sensitive elements to refine the piece part calibration model. Sometimes heating and cooling of various subassemblies (waveguide, OMT, and circulator) is used to verify their effect on the radiometer output during the system test if layout permits. One approach to minimize errors in this type of calibration system is to make all of these critical calibration path components nearly isothermal at a fixed temperature by active thermal control. Care must also be taken to prevent thermal IR energy from entering the calibration paths via the cold horns and feed horns and causing localized heating of critical calibration elements.

A second calibration approach not used in the LAMMR baseline design provides the calibration sources through the same transmission path as the primary scene radiation coming from the ground. This is the technique used in the Nimbus 6 SCAMS, TIROS-N MSU, and most small aperture radiometer systems where the scanning apertures view cold space and warm black body targets during a calibration cycle. In some cases two black body targets are used with the temperatures separated by  $\sim 100\text{K}$ . Space radiation cooling techniques can be used to lower the black body temperatures to  $\sim 200\text{K}$ , but the cooling apertures required make these systems large. The LAMMR conical scan geometry makes viewing space with the full aperture impossible during normal operation, but secondary reflectors can be used in front of the feeds to view cold space (ref. HRMI Final Report, GE No. 7850 S425, Nov. 1979). The clear calibration algorithm advantages of viewing the two calibration sources through the same transmission line must be traded off against the mechanisms, black body sizes, and space view subreflectors required to implement such a system with the relatively large prime focus LAMMR feed cluster. This "feed viewing calibration source" technique has the additional advantage of eliminating the need for any ferrite switches in front of a total power radiometer. These switches are significant loss elements which add to the system noise temperature raising  $\Delta T$ . They can also introduce changes in isolation and losses over normal spacecraft temperature ranges (ref. NASA TM-80244, C. D. Calhoun, March 1979) as discussed earlier.

#### IV. LAMMR ANTENNA SUBSYSTEM

The baseline LAMMR antenna system concept consists of an offset parabolic reflector with clustered feed horns located on a deployable arm. The scan mechanism continuously rotates the antenna and radiometer subsystem at one revolution per second. The offset reflector will have a projected circular aperture of approximately 4 meters as shown in Figure 10. The actual shape of the reflector through the truncation plane is elliptical and the major and minor axis dimensions depends on the  $f/D$  and offset of the projected circular aperture from the focal axis ( $f$  = focal distance,  $D$  = aperture diameter in Figure 10). This offset is selected to allow the feeds and radiometer electronics to be located at the focal point without causing any blockage to the projected aperture. The feeds which are clustered around the focus are pointed at the offset section near the center of the surface. The optimization of these angles  $\phi$  and  $\theta$  influence the polarization isolation and secondary pattern performance of the antenna system and larger  $f/D$  ratios improve clustered feed pattern performance.<sup>3</sup> The reflector  $f/D$  ratio and offset are performance variables which must be optimized for both electrical antenna performance and system dynamic spin balance. The mechanical spin axis is inclined approximately 43 degrees (see Figure 5) to the antenna beam pattern axis and the intersection of this axis with the reflector surface is selected to achieve dynamic balance of the spinning antenna/radiometer subsystems. The summation of the radial forces on the feed arm can also be minimized by prudent selection of the  $f/D$  ratio and spin axis location. In fact, the selection of the prime focus .66  $f/D$  system over a Cassegrain feed approach with a much shorter feed arm was made because of this dynamic balance consideration during the phase B studies by GE and AES. Cassegrain feed spillover which viewed the earth was also a negative factor used in selecting the prime focus feed approach where spillover views cold space or possibly the spacecraft. The LAMMR antenna system performance requirements are outlined in Figure 9. One apparent unusual requirement of the LAMMR antenna system is to maintain the same .26° elevation plane beamwidth from 36.5 to 91 GHz. This requires the higher frequency channel feed horns to under-illuminate the reflector effectively viewing only approximately 2.3 meters at 36.5 GHz and approximately 1 meter at 91 GHz. The under-illumination requirement makes the sizes of the horns larger which pushes



**FEED POINTING  
AXIS**

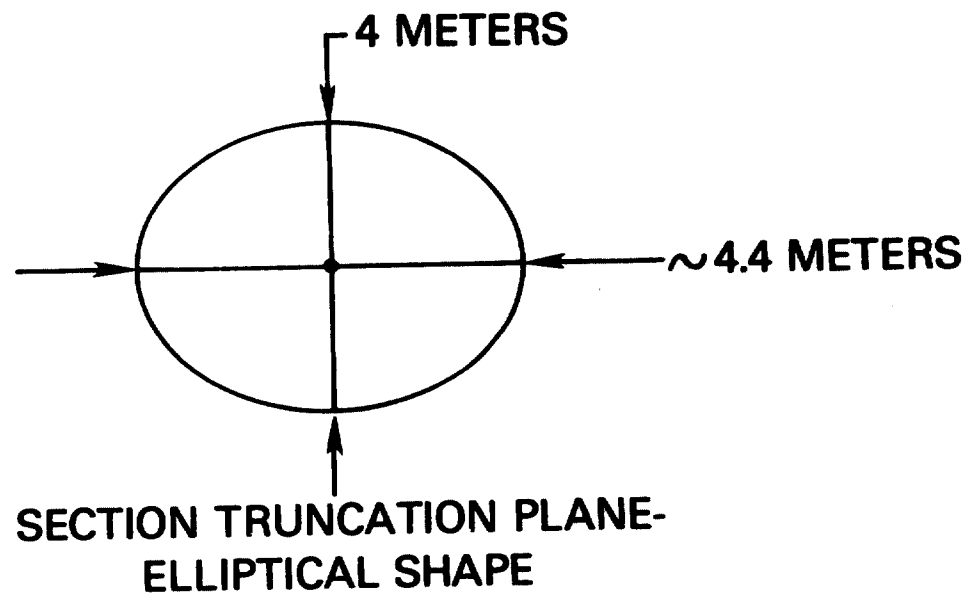


Figure 10. LAMMR Antenna Geometry

the outside clustered feed more off axis and degrades performance. Defocussing of the feeds is another concept for increasing the beamwidth and a combination of these two approaches is also possible. The combination of two or more frequencies in a common feed horn as was done on the Nimbus-7 Scanning Multichannel Microwave Radiometer (5 frequencies) is also possible depending on the frequency separation and required illumination tapers. The combined single horn approach must be traded off against increased losses, horn complexity and size when making the final horn design selection. The present baseline LAMMR feed design uses separate multimode horns for all channels. The choice of multimode  $TE_{11}/TM_{11}$  horns over corrugated horns was made because the smaller size of the multimode horns made the feed cluster more compact around the focal point. This more compact feed cluster improves beam efficiency by minimizing coma lobe energy due to focal point offsets. The multimode horns have the additional benefit over corrugated designs because they are easier to fabricate which makes them less expensive.

Antenna beam efficiency  $\eta_B$  is a very important antenna performance requirement for microwave radiometer systems which must be traded off against minimum beamwidth and aperture efficiency. The 90%  $\eta_B$  specification is defined as all of the energy contained within the first antenna pattern null or 2.5 times the 3 db beamwidth (whichever is smaller) over all of the integrated energy (see NASA TM-80603, R. F. Schmidt, Dec. 1979, for more detailed definition). This is critical because of the requirement to detect small temperature gradients with the antenna beams in the ocean and ice canopies near land and precipitation features which are much higher in brightness temperature  $T_B$ . The influence of these adjacent cells must be corrected in the data processing phase even with very high beam efficiencies, but this would be impossible with low (approximately 50-60%) beam efficiencies and the system measurement errors would increase significantly if the 90% efficiencies are not achieved.

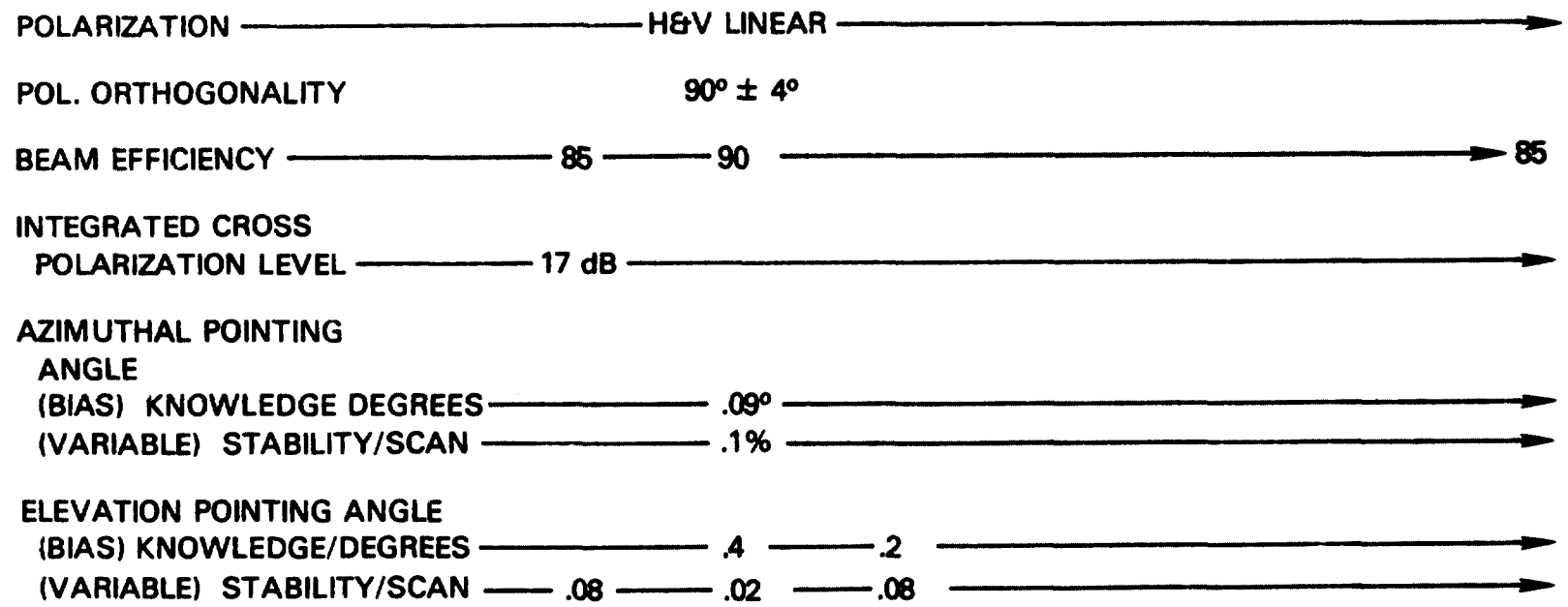
The beam efficiency is controlled primarily by two parameters in an unblocked reflector system: the feed illumination taper and the RMS surface tolerance of the reflector surface. The feed illumination tapers must be in the 16-20 db region to achieve this level of  $\eta_B$  performance. The

reflector surface tolerance requirements are more difficult to specify although the  $1/32 \lambda$  Ruze equation requirement is often used. At the one revolution per second scan rate the LAMMR reflector assumes an S shaped distortion which can exceed the Ruze equation  $1/32 \lambda$  requirement without major impacts on beam efficiency. (Ref.: NASA TM 80687, L. R. Dod, LAMMR Antenna Design, May 1980.) The calculated tip deflections using NASTRAN structural models of the graphite honeycomb reflectors were in the order of  $25 \times 10^{-3}$  cm (10 mil inches) with much smaller deflectors approximately  $5 \times 10^{-3}$  cm (2 mil inches) near the center of the reflector in the hub attachment region where the high frequency channels are using the reflector with high feed illumination energy levels. These reflector deflections were analytically modelled and secondary patterns generated which showed an approximately 2% decrease in beam efficiency due to these distortions (Ref.: TM 80687). These reflector and feed analytical models (GSFC, GE and AES) have shown the feasibility of designing and developing the critical LAMMR antenna/feed assembly which can be rotated at 1 revolution per second with the beamwidths and beam efficiencies shown in Figure 11.

## V. CONCLUSION

This TM has presented the LAMMR baseline design and system design tradeoff rationale in a few illustrative areas which are critical to the system's electrical performance. The LAMMR is a state-of-the-art electromechanical system. Extensive mechanical scan subsystem design tradeoffs which affect the scan motion and spacecraft torque jitter interface are not presented in this TM. These scan mechanism tradeoffs were made by the two phase B study contractors which show compatibility with free flyer spacecraft and the details can be found in their reports. Analytical models of both the structure and antenna performance developed by GSFC, GE, and AES during the studies were the main source of the quantitative data base from which many of these baseline design conclusions have been made. These results show the feasibility of developing a flight model LAMMR of this baseline configuration in 3 to 4 years, but we also acknowledge that the LAMMR sensor development into a spacecraft system is an ambitious undertaking with significant engineering challenges which could change this baseline concept. This is particularly true because of the undefined nature

CHANNEL GHz	1.4	4.3	10.65	18.7	21.3	36.5	91
BANDWIDTH	28 MHz	200 MHz	100 MHz	200 MHz	200 MHz	1000 GHz	2400 MHz
BEAMWIDTH DEGREES	3.8	1.3	.6	.3	.26	.26	.26



26

Figure 11. LAMMR Antenna System Requirements



of the NOSS spacecraft at this time and some changes in the LAMMR/spacecraft interfaces. The demand for the LAMMR data products (sea surface temperature, wind speed, sea ice concentration, etc.) by various user agencies (DoD, NOAA, USGS, etc.) show a strong belief in the potential usefulness of this more accurate high resolution information which warrants the development risks and system costs which will be incurred over the next 5 years.

The broad NOSS program objective is the development and limited operational demonstration of a remote sensing system which will supply specific global oceanographic data under all weather conditions on a routine and repetitive basis. If successful, the NOSS series will probably evolve into a full-time operational observing system similar to the TIROS/NOAA weather satellites.

#### ACKNOWLEDGEMENTS

The author acknowledges many helpful discussions with Dr. J. Eckerman, Dr. T. T. Wilheit, and W. T. Walton concerning the contents of this TM. He also acknowledges the critical technical contributions of the Goddard, General Electric, and Aerojet Electro System Study Teams in analyzing the LAMMR subsystem performance which has been used to describe the rationale for the present LAMMR baseline system.

#### REFERENCES

1. John C. Alishouse, Washington, D.C., NOAA Technical Memo NESS 66: A Summary of the Radiometric Technology Model of the Ocean Surface in the Microwave Region, March 1975.
2. Wilheit, NASA TM 80278: A Model for the Microwave Emissivity of the Ocean's Surface as a Function of Wind Speed, April 1979.
3. R. F. Schmidt, NASA Technical Memo 80603, Alternative Beam Efficiency Calculations for a Large-Aperture Multi-Frequency Microwave Radiometer (LAMMR), December 1979.